

M. Khalid Aurangzaib*, Krishnendu Bhattacharyya, and Sharidan Shafie

Multiple Solutions of an Unsteady Stagnation-Point Flow with Melting Heat Transfer in a Darcy–Brinkman Porous Medium

DOI 10.1515/nleng-2015-0034

Received November 19, 2015; accepted January 30, 2016.

Abstract: The characteristics of the unsteady boundary layer flow with melting heat transfer near a stagnation-point towards a flat plate embedded in a Darcy-Brinkman porous medium with thermal radiation are investigated. The governing partial differential equations are transformed into self-similar ordinary differential equations by similarity transformations. The transformed self-similar equations are solved numerically using `bvp4c` from Matlab for several values of the flow parameters. The study reveals that the multiple solutions exist for the decelerating ($A < 0$) flow, whereas for the accelerating ($A \geq 0$) flow, the solution is unique. The results also indicate that the melting phenomenon increases the rate of heat transfer and delays the boundary layer separation. To validate the current numerical results, comparison with available results is made and found to be in a good agreement.

Keywords: Unsteady flow; melting heat transfer; porous medium

PACS: 44.20.+b; 44.30.+v; 44.40.+a; 47.15.Cb

1 Introduction

The study of boundary layer flow and heat transfer through a porous medium is significance in several practical fields, especially in field of agriculture and in petroleum technology. A better understanding of convection through porous

medium can benefit several areas like insulation design, grain storage, geothermal systems, heat exchangers, filtering devices, metal processing, catalytic reactors etc [1]. More details on this topic and its applications can be found in books by Pop and Ingham [2], Ingham et al. [3], Bejan et al. [4], Vafai [5], Ingham and Pop [6], Nield and Bejan [7] and Vadasz [8]. It is well known that Darcy's law is an empirical formula relating the pressure gradient, the bulk viscous fluid resistance and the gravitational force for a forced convective flow in a porous medium. Deviations from Darcy's law occur when the Reynolds number based on the pore diameter is within the range of 1 to 10 [9]. However, the boundary and inertia effects which are not included in Darcy's model, may modify the flow and heat transfer characteristics. Therefore, it is essential to determine the conditions under which these effects are important. Harris et al. [10] used the Brinkman slip model to study the mixed convection flow towards a stagnation-point past a vertical surface immersed in a porous medium. The boundary layer flow of a nanofluid towards a stagnation-point over a stretching sheet in a porous medium with heat generation/absorption was investigated by Hamad and Pop [11]. Rosali et al. [12] used the Brinkman-extended model to study the mixed convective stagnation-point flow towards a vertical plate embedded in a porous medium with heat flux and obtained dual solutions for assisting and opposing flows. Pantokratoras [13] obtained non-similar solutions of the mixed convection boundary layer flow and heat transfer embedded in Darcy-Brinkman porous medium in the presence of convective boundary condition. Recently, Pantokratoras [14] investigated the forced convective flow with heat transfer in a Darcy-Brinkman porous medium with convective boundary condition.

Recently, the heat transfer accompanied with melting (or solidification) effect received numerous interests in the area of magma solidification, the melting of permafrost, and silicon wafer process [15]. Epstein and Cho [16] studied the laminar flow with melting heat transfer past a flat plate. Kazmierczak et al. [17] studied the natural convection flow with melting heat transfer over a vertical flat

*Corresponding Author: M. Khalid Aurangzaib: Department of Mathematical Sciences, Federal Urdu University of Arts, Science & Technology, Gulshan-e-Iqbal Karachi, Pakistan, E-mail: zaib20042002@yahoo.com

Krishnendu Bhattacharyya: Department of Mathematics, The University of Burdwan, Burdwan 713104, West Bengal, India

Sharidan Shafie: Department of Mathematical Sciences, Faculty of Science, Universiti Teknologi Malaysia JB, 81310 Skudai, Johor, Malaysia

plate in a porous medium. The steady boundary layer flow with melting heat transfer past a moving surface was investigated by Ishak et al. [18]. Hayat et al. [19] studied the boundary layer flow of couple stress fluid near a stagnation-point with melting heat transfer towards a stretching sheet. Recently, Ahmad and Pop [20] investigated the steady mixed convection flow with melting heat transfer over a vertical surface in a porous medium and obtained dual solutions for opposing flow only. Very recently, Mabood and Mastroberardino [21] studied the melting effect on MHD flow of a nanofluid towards a stretching sheet in the presence of viscous dissipation and second order slip effects.

In most cases, the solution of unsteady Navier–Stokes equations can be obtained only by using numerical integrations of the partial differential equation. But, if the motion is restricted to a specified family of time dependence, exact similarity solutions can be achieved as was shown by Yang [22] and Birkhoff [23]. The form given by the relation $u_e(x, t) = ax/(1 - ct)$ was used here by Yang [22] for the outer flow and referred to as hyperbolic time variation. This form of relation has been also used by many researchers such as Wang [24]; Andersson et al. [25]; Ali and Magyari [26]; Tie-Gang et al. [27]. Rohni et al. [28] used the Darcy slip model to investigate the unsteady mixed convection flow near a stagnation-point towards a porous vertical surface embedded in a porous medium. Recently, Sheremet and Trifonova [29] investigated unsteady natural convection flow over a vertical cylinder including horizontal porous layer. They considered both Darcy and Brinkman-extended Darcy models.

To the author's best of knowledge the unsteady boundary layer flow with melting heat transfer near a stagnation-point embedded in Darcy-Brinkman porous medium with thermal radiation has not been considered yet and this is the target of the current work. Numerical results of the self-similar ordinary differential equations are obtained using bvp4c function from Matlab.

2 Problem Formulation

Consider an unsteady two-dimensional incompressible viscous fluid near a stagnation-point past a flat plate embedded in a Darcy Brinkman porous medium with melting and radiation effects as shown in Figure 1. The external flow velocity is assumed to vary linearly in the form of $u_e(x, t) = ax/(1 - ct)$, where both a and c are positive constants with dimensions T^{-1} with c showing the unsteadiness of the problem. It is also assumed that the tempera-

ture of melting surface is T_m , while the free stream temperature is T_∞ , where $T_\infty > T_m$. Under these assumptions along with the usual boundary layer, the governing equations are

$$\frac{\partial u}{\partial x} + \frac{\partial v}{\partial y} = 0 \quad (1)$$

$$\frac{\partial u}{\partial t} + u \frac{\partial u}{\partial x} + v \frac{\partial u}{\partial y} = \frac{\partial u_e}{\partial t} + u_e \frac{\partial u_e}{\partial x} + \varepsilon^2 v_{eff} \frac{\partial^2 u}{\partial y^2} + \frac{\varepsilon^2 v}{K_1} (u_e - u) \quad (2)$$

$$\frac{\partial T}{\partial t} + u \frac{\partial T}{\partial x} + v \frac{\partial T}{\partial y} = \alpha \frac{\partial^2 T}{\partial y^2} - \frac{1}{\rho c_p} \frac{\partial q_r}{\partial y} \quad (3)$$

The corresponding boundary conditions are

$$\begin{aligned} t < 0 : u &= 0, v = 0, T = T_\infty \quad \text{for all } x, y, \\ t \geq 0 : u &= 0, v = 0, T = T_m \text{ at } y = 0, \\ u &\rightarrow u_e(x, t), T \rightarrow T_\infty \text{ as } y \rightarrow \infty, \end{aligned} \quad (4)$$

and

$$k \left(\frac{\partial T}{\partial y} \right)_{y=0} = \rho [\lambda + c_s(T_m - T_0)] v(x, 0, t). \quad (5)$$

where u and v are velocity components in x and y directions respectively, ν is the kinematic fluid viscosity, ρ is the density, $\nu_{eff} = \mu_{eff}/\rho$ is the effective kinematic viscosity, μ_{eff} is the effective (or “apparent”) viscosity, ρ is the fluid density, g is the acceleration due to gravity, k is the thermal conductivity, α is the thermal diffusivity, c_p is the specific heat, ε is the porosity of the porous medium, K_1 is the permeability of the porous medium, T is the temperature, T_∞ is the ambient temperature, c_s is the heat capacity of the solid surface, λ is the latent heat of fluid, T_0 is the surface temperature and T_m is the melting temperature.

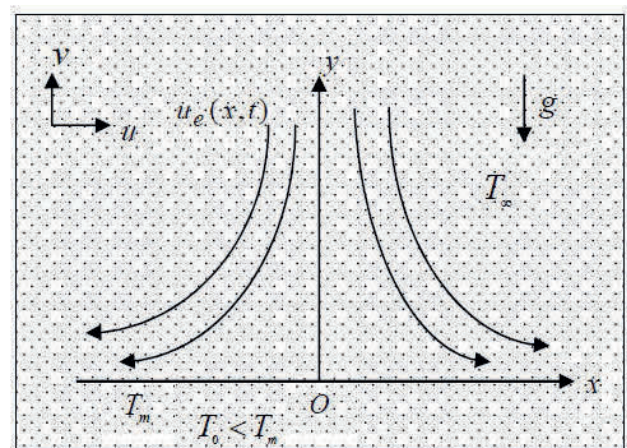


Fig. 1: The physical model and coordinate system

Using Rosseland's approximation for radiation (Brewster [30]), we have

$$q_r = -\frac{4\sigma^*}{3k^*} \frac{\partial T^4}{\partial y}, \quad (6)$$

where σ^* is the Stefan-Boltzman constant, k^* is the absorption coefficient. We suppose that the temperature variation within the flow is such that T^4 may be expanded in a Taylor's series. Expanding T^4 about T_∞ and neglecting higher order terms we get,

$$T^4 \cong 4T_\infty^3 T - 3T_\infty^4. \quad (7)$$

Therefore, equation (3) reduces to

$$\frac{\partial T}{\partial t} + u \frac{\partial T}{\partial x} + v \frac{\partial T}{\partial y} = \alpha \frac{\partial^2 T}{\partial y^2} + \frac{16\sigma^* T_\infty^3}{3k^* \rho c_p} \frac{\partial^2 T}{\partial y^2} \quad (8)$$

Introducing the following similarity transformation (Rosali et al. [12]; Rohni et al. [28])

$$\begin{aligned} \eta &= y \sqrt{\frac{a}{\alpha(1-ct)}}, \\ \psi &= \sqrt{\frac{a\alpha}{(1-ct)}} x f(\eta), \\ \theta(\eta) &= \frac{T - T_m}{T_\infty - T_m}, \quad K_1 = K^* (1 - ct) \end{aligned} \quad (9)$$

Using (9), the equation of continuity (1) is automatically satisfied and the nonlinear partial differential equations (2) and (8) are transformed into the following ordinary differential equations

$$\Lambda f'''' + ff'' - f'^2 - A \left(f' + \frac{1}{2} \eta f'' - 1 \right) + K(1 - f') + 1 = 0 \quad (10)$$

$$\theta'' + \left(\frac{3N}{3N+4} \right) \left\{ f\theta' - \frac{1}{2} A \eta \theta' \right\} = 0 \quad (11)$$

The transformed boundary condition are

$$\begin{aligned} f'(0) &= 0, \quad f(0) + M\theta'(0) = 0, \quad \theta(0) = 0 \\ f'(\infty) &= 1, \quad \theta(\infty) = 1 \end{aligned} \quad (12)$$

where prime denote differentiation with respect to η , $\Lambda = \varepsilon^2 v_{eff}/\alpha = \varepsilon^2 \text{Pr}$ is the modified porosity parameter, $K = v\varepsilon^2/aK^*$ is the dimensionless permeability parameter, $A = c/a$ is the unsteady parameter, $M = c_f(T_\infty - T_m)/[\lambda + c_s(T_m - T_0)]$ is the dimensionless melting parameter and $N = k^*k/4\sigma T_\infty^3$ is the radiation parameter.

The physical quantity of interest are the skin friction coefficient and the local Nusselt number which are defined as

$$C_f = \frac{\tau_w}{\rho u_e^2/2}, \quad Nu_x = \frac{xq_w}{k(T_\infty - T_m)} \quad (13)$$

where τ_w is the shear stress and q_w is the heat flux which are defined as

$$\tau_w = \mu \left(\frac{\partial u}{\partial y} \right)_{y=0}, \quad q_w = -k \left(\left(1 + \frac{16\sigma^* T_\infty^3}{3k^*} \right) \frac{\partial T}{\partial y} \right)_{y=0} \quad (14)$$

Therefore, we get the wall skin friction coefficient C_f and the local Nusselt number Nu_x as follows:

$$\frac{1}{2} C_f Re_x^{1/2} / \text{Pr} = f''(0), \quad Nu_x / Pe_x^{1/2} = - \left(\frac{3N+4}{3N} \right) \theta'(0) \quad (15)$$

where $Re_x = xu_e/\nu$ is the local Reynolds number and $Pe_x = xu_e/\alpha$ is the local Péclet number.

3 Stability Analysis

Dual solutions are categorized as upper branch solution (first solution), and lower branch (second solution). There are several researchers such as Weidman et al. [31], Roşca and Pop [32], Mahapatra and Nandy [33], Nazar et al. [34] and recently, Hafidzuddin et al. [35] have performed stability analysis to determine which solution is stable. They have shown in these papers that the second (lower branch) solutions are unstable, whilst the first (upper branch) solutions are stable and physically reliable. Following Weidman et al. [31], a new dimensionless time variable τ is introduced. The use of τ is associated with an initial value problem and is consistent with the question of which solution or branch will be obtained in practice (physically reliable).

With an introduction of τ and (9), we have

$$\begin{aligned} u &= \frac{ax}{1-ct} f'(\eta, \tau), \quad v = \sqrt{\frac{a\alpha}{1-ct}} f(\eta, \tau), \quad \eta = y \sqrt{\frac{a}{\alpha(1-ct)}}, \\ \tau &= \frac{at}{1-ct} \quad T - T_m = (T_\infty - T_m) \theta(\eta, \tau), \quad K_1 = K^* (1 - ct) \end{aligned} \quad (16)$$

Substituting (16) into (2) and (8), we get the following:

$$\begin{aligned} \Lambda \frac{\partial^3 f}{\partial \eta^3} + f \frac{\partial^2 f}{\partial \eta^2} - \left(\frac{\partial f}{\partial \eta} \right)^2 - A \left(\frac{\partial f}{\partial \eta} + \frac{1}{2} \eta \frac{\partial^2 f}{\partial \eta^2} - 1 \right) \\ + K \left(1 - \frac{\partial f}{\partial \eta} \right) + 1 - \frac{1}{1-ct} \frac{\partial^2 f}{\partial \eta \partial \tau} = 0 \end{aligned} \quad (17)$$

$$\frac{\partial^2 \theta}{\partial \eta^2} + \left(\frac{3N}{3N+4} \right) \left\{ f \frac{\partial \theta}{\partial \eta} - \frac{1}{2} A \eta \frac{\partial \theta}{\partial \eta} - \frac{1}{1-ct} \frac{\partial \theta}{\partial \tau} \right\} = 0 \quad (18)$$

subject to the following boundary conditions

$$\begin{aligned} \frac{\partial f}{\partial \eta}(0, \tau) &= 0, \quad f(0, \tau) = M \frac{\partial \theta(0, \tau)}{\partial \eta}, \\ \theta(0, \tau) &= 0 \frac{\partial f(\eta, \tau)}{\partial \eta} \rightarrow 1, \quad \theta(\eta, \tau) \rightarrow 1 \text{ as } \eta \rightarrow \infty \end{aligned} \quad (19)$$

To test the stability of the steady flow solution $f(\eta) = f_0(\eta)$ and $\theta(\eta) = \theta_0(\eta)$ satisfying the boundary value problem (1)-(5), we can write

$$\begin{aligned} f(\eta, \tau) &= f_0(\eta) + e^{-\beta\tau} F(\eta, \tau), \\ \theta(\eta, \tau) &= \theta_0(\eta) + e^{-\beta\tau} G(\eta, \tau), \end{aligned} \quad (20)$$

where β is an unknown eigenvalue, $F(\eta, \tau)$ and $G(\eta, \tau)$ are small relative to $f_0(\eta)$ and $\theta_0(\eta)$. Substituting (20) into (17) and (18), we get the following linearised equations

$$\begin{aligned} \Lambda \frac{\partial^3 f}{\partial \eta^3} + f_0 \frac{\partial^2 F}{\partial \eta^2} - f_0' F - (2f_0' - (1 + A\tau)\beta) \frac{\partial F}{\partial \eta} \\ - A \left(\frac{\partial F}{\partial \eta} + \frac{1}{2} \eta \frac{\partial^2 F}{\partial \eta^2} \right) - K \frac{\partial F}{\partial \eta} - (1 + A\tau) \frac{\partial^2 F}{\partial \eta \partial \tau} = 0 \end{aligned} \quad (21)$$

$$\begin{aligned} \left(\frac{3N+4}{3N} \right) \frac{\partial^2 G}{\partial \eta^2} + f_0 \frac{\partial G}{\partial \eta} + F\theta_0' - \frac{1}{2} A\eta \frac{\partial G}{\partial \eta} + (1 + A\tau)\beta G \\ - (1 + A\tau) \frac{\partial G}{\partial \tau} = 0 \end{aligned} \quad (22)$$

along with the following boundary conditions

$$\begin{aligned} \frac{\partial F}{\partial \eta}(0, \tau) = 0, \quad F(0, \tau) = M \frac{\partial G(0, \tau)}{\partial \eta}, \\ G(0, \tau) = 0 \frac{\partial F(\eta, \tau)}{\partial \eta} \rightarrow 0, \quad G(\eta, \tau) \rightarrow 0 \text{ as } \eta \rightarrow \infty \end{aligned} \quad (23)$$

As proposed by Weidman et al. [31], we analyze the stability of the steady flow and heat transfer solution $f_0(\eta)$ and $\theta_0(\eta)$ by setting $\tau = 0$, and thus $F = F_0(\eta)$ and $G = G_0(\eta)$ in (21) and (22) to identify initial growth or decay of the solution (20). To test our numerical procedure we have to solve the linear eigenvalue problem

$$\Lambda F_0''' + f_0 F_0'' - f_0' F_0 - (2f_0' - \beta) F_0 - A \left(F_0' + \frac{1}{2} \eta F_0'' \right) - K F_0' = 0 \quad (24)$$

$$\left(\frac{3N+4}{3N} \right) G_0'' + f_0 G_0' + F_0 \theta_0' - \frac{1}{2} A \eta G_0' + \beta G_0 = 0 \quad (25)$$

along with the following boundary conditions

$$\begin{aligned} F_0'(0) = 0, \quad F_0(0) = M G_0'(0), \quad G_0(0) = 0 \\ F_0'(\eta) \rightarrow 0, \quad G_0(\eta) \rightarrow 0 \text{ as } \eta \rightarrow \infty \end{aligned} \quad (26)$$

It is worth mentioning that for a particular values of physical parameters Λ, β, A, K and N the corresponding steady flow solution $f_0(\eta)$ and $g_0(\eta)$, the stability of the steady flow solution is determined by the smallest eigenvalue β . Solutions of the problem (20) and (21) give an infinite set of eigenvalues $\beta_1 < \beta_2 < \beta_3 < \dots$; if the smallest eigenvalue β_1 is positive ($\beta_1 \geq 0$) then there is an initial decay

of disturbances and the flow is stable, and if β_1 is negative ($\beta_1 < 0$) then there is an initial growth of disturbances, which indicates that the flow is unstable. As suggested by Harris et al. [36], the range of possible eigenvalues can be obtained by relaxing a boundary condition on $F_0(\eta)$ or $G_0(\eta)$. For the current problem, we relax the condition $G_0(\eta) \rightarrow 0$ as $\eta \rightarrow \infty$ and for a fixed value of β , we solve the system of equations (24) and (25) subject to the boundary conditions (26), along with the new boundary condition $G_0'(0) = 1$.

4 Results and Discussion

The set of transformed nonlinear differential equations (10) and (11) along with the boundary conditions (12) were solved numerically using the bvp4c code from Matlab. To clearly realize physical insight for melting heat transfer characteristics in presence of radiation effect, the obtained numerical results for the skin friction coefficient, the heat transfer rate as well as for velocity and temperature profiles are plotted for different values of physical parameters encountered in the problem, viz., the melting parameter (M), unsteady parameter (A), the radiation parameter (N), permeability parameter (K) and modified porosity parameter (Λ) in Figures 2–14. The accuracy of our numerical results is checked with the results of Yih [37] and Ishak et al. [38] for the reduced skin friction in the limiting case. Thus, it is seen from Table 1 that the numerical results are in good agreement with those published previously. This validated the accuracy of the present results.

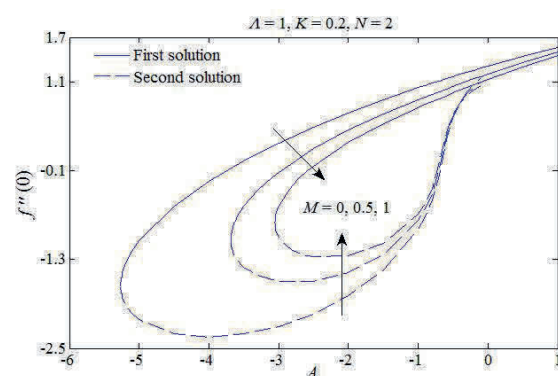


Fig. 2: The Skin friction coefficient $f''(0)$ with A for different values of M .

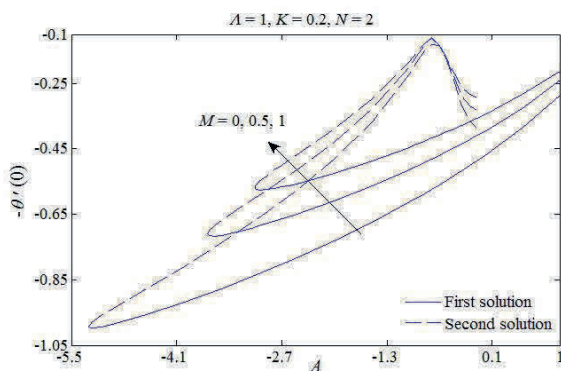
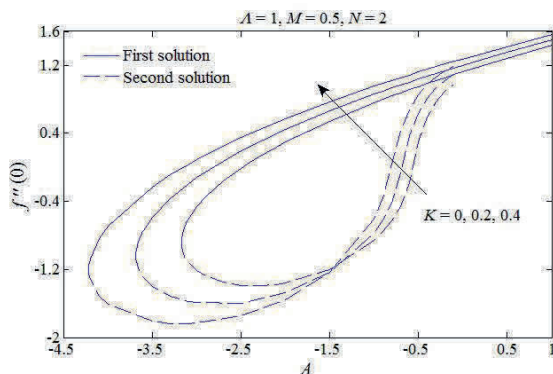
The variation of the skin friction $f''(0)$ and heat transfer rate $-\theta'(0)$ with unsteady parameter A for various values of M are shown in Figs. 2 and 3. From these figures,

Table 1: Comparison of results for $f''(0)$ when $\Lambda = 1$, $M = K = A = 0$.

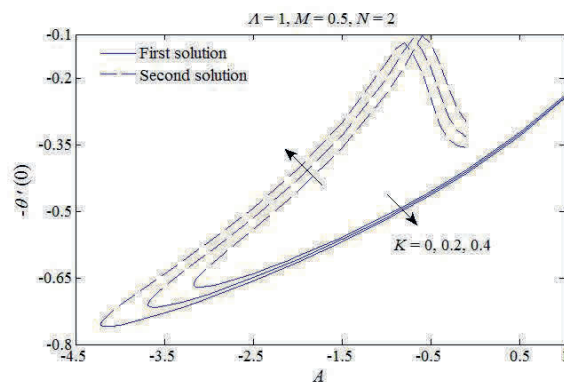
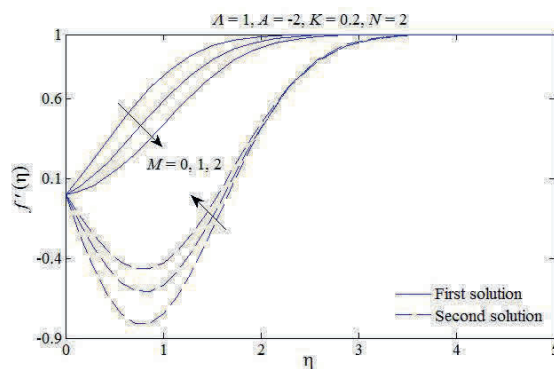
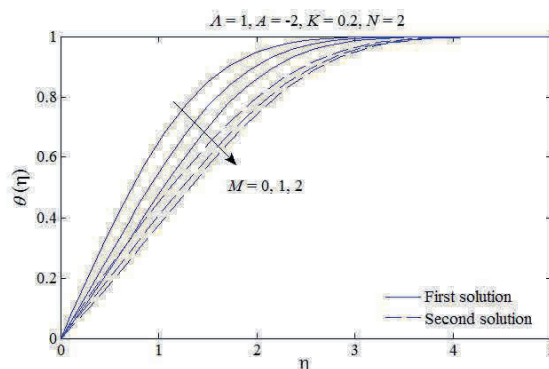
Yih [37]	Ishak et al. [38]	Present results
1.232588	1.2326	1.2326

Table 2: Values of A_{\min} for different values of K when $\Lambda = 1$, $M = 0.5$, $N = 2$.

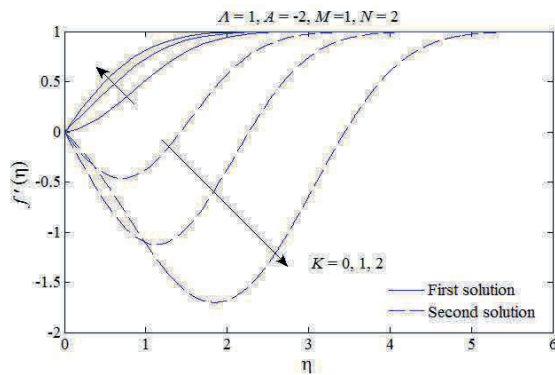
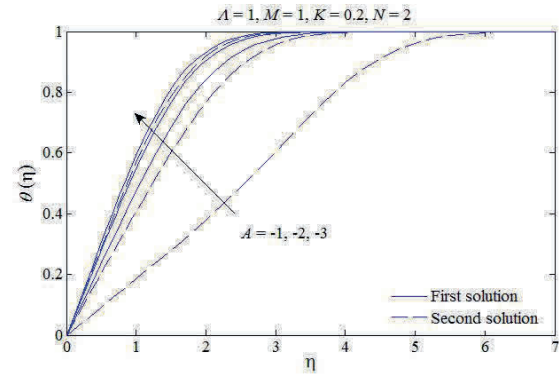
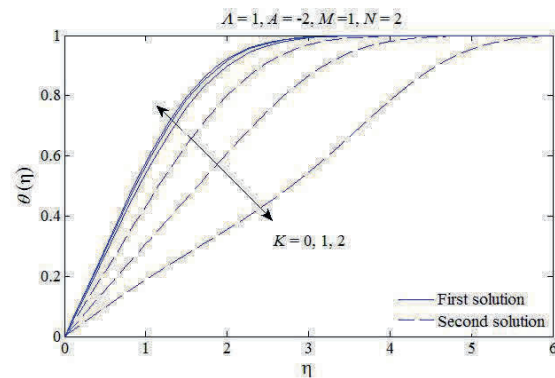
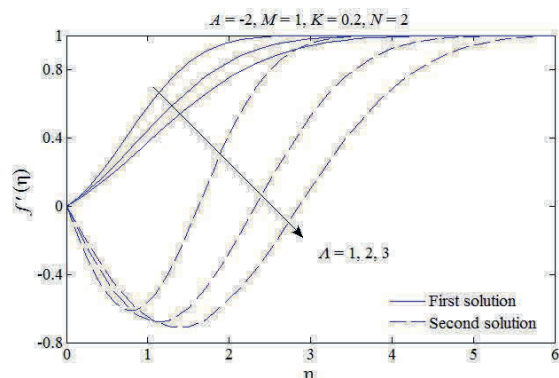
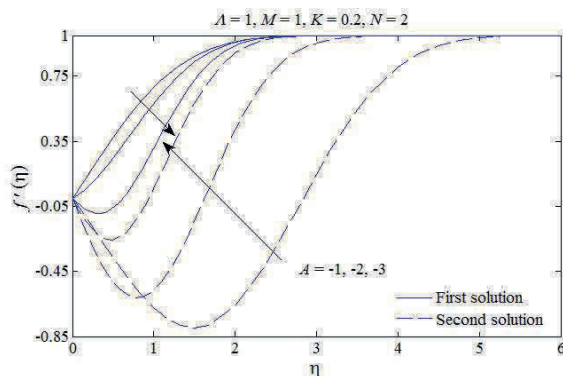
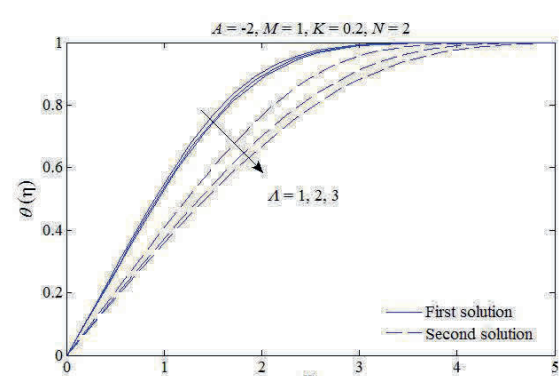
K	0	0.2	0.4
A_{\min}	-3.1720	-3.6850	-4.2151
$f''(0)$	-0.8835	-1.0380	-1.2023
$-\theta'(0)$	-0.6643	-0.7096	-0.7538

**Fig. 3:** The heat transfer rate $-\theta'(0)$ with A for different values of M .**Fig. 4:** The Skin friction coefficient $f''(0)$ with A for different values of K .

it can be observed that multiple solutions of self-similarity equations (10) and (11) subjected to (12) exist in decelerating flow ($A < 0$), while for accelerating flow ($A \geq 0$), the solution is unique. On the other hand, the dual similarity solutions (similarity solution for steady case) are obtained for $A \geq A_{\min}$ and the flow has no solution for $A < A_{\min}$, where A_{\min} is the critical value of A . For $M = 0$, the flow has a similarity solution for $A \geq -5.2670$ and consequently for $A < -5.2670$ no similarity solution exists. For $M = 0.5$, the

**Fig. 5:** The heat transfer rate $-\theta'(0)$ with A for different values of K .**Fig. 6:** Velocity profiles for different values of M .**Fig. 7:** Temperature profiles for different values of M .

similarity solutions exist for ranges of A is $A \geq -3.6850$ and hence no similarity solution exists for $A < -3.6850$. Further, it is interesting to note that more increment in melting parameter M causes more reduction ($|A_{\min}|$) in the solution domain. For $M = 1$, the similarity solution exists when $A \geq -3.0530$ and thus no solution exists for $A < -3.0530$. It is also seen from these results that the first solution makes a U-turn at this point and continues to the second solution. The second solutions continue further and terminate at certain values of A . Fig. 2 shows that

Fig. 8: Velocity profiles for different values of K .Fig. 11: Temperature profiles for different values of A .Fig. 9: Temperature profiles for different values of K .Fig. 12: Velocity profiles for different values of A .Fig. 10: Velocity profiles for different values of A .Fig. 13: Temperature profiles for different values of A .

the values of $f''(0)$ decreases with increasing M for first solution, while the values increases in case of second solution. Whereas, the values of $-\theta'(0)$ increases with M for both first and second solutions as shown in Fig. 3.

Figures 4 and 5 illustrate the variation of $f''(0)$ and $-\theta'(0)$ versus A for different values of permeability parameter K . Fig. 4 shows that the values of $f''(0)$ increases with increasing K for first and second solutions, whereas the heat transfer rate decreases with increasing K for first solution and increases in case of second solution as shown

in Fig. 5. Further, Figs. 4 and 5 and Table 2 show that the minimum (critical) value $|A_{\min}|$ increases when the permeability parameter K increases, and this suggests that permeability increases the range of existence of the solutions. Moreover, the values of heat transfer rate is negative (Fig. 5), which implies that heat is transformed from cold fluid to hot surface.

The velocity and temperature profiles for different values of melting parameter M are depicted in Figs. 6 and 7. Fig. 6 shows that the velocity profiles decreases with in-

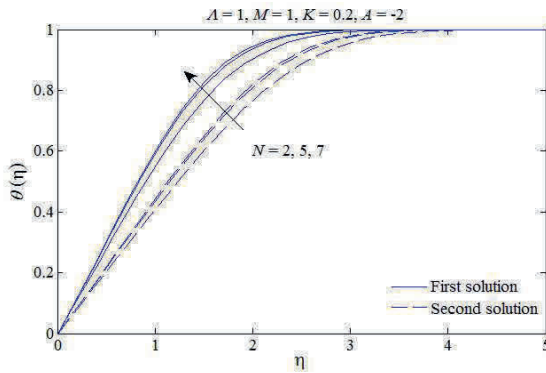


Fig. 14: Temperature profiles for different values of N .

creasing M for first solution and consequently increases the thickness of momentum boundary layer. While, the opposite trend is observed for second solution. On the other hand, the temperature of fluid decreases with increasing M for first and second solutions as shown in Fig. 7. Thus the thermal boundary thickness become thicker and thicker for both solutions. This is due to the fact that the temperature difference between ambient and melting surface increases which enhances the velocity and reduces the temperature of fluid.

Figures 8 and 9 illustrated the effect of permeability parameter K on the velocity and temperature profiles. From these figures, it is observed that the velocity and temperature profiles increase with K for first solution and hence the boundary layer thicknesses become thinner and thinner. Whereas, the opposite trend is observed in case of second solution. With a rise in permeability of the medium, the regime becomes more porous. As a consequence, the Darcian body force decreases in magnitude (as it is inversely proportional to the permeability). The Darcian resistance acts to decelerate the fluid particles in continua. This resistance diminishes as permeability of the medium increases. So progressively less drag is experienced by the flow and flow retardation is thereby decreased. Thus the permeability parameter enhances the fluid motion inside the boundary layer. It is also seen from these figures that the second solutions have larger boundary layer thickness compared to the first solutions. Both the solutions satisfy the far field boundary conditions asymptotically, and thus mathematically could not be neglected.

The effect of unsteady parameter A on the velocity and temperature profiles is illustrated in Figs. 10 and 11. The effect of unsteady parameter A is major in second solution branch. From Fig. 10, it is observed that the velocity boundary layer thickness decreases with increasing values of unsteady parameter $|A|$ in first solution, while the op-

posite effect is observed in second solution. Fig. 11 shows that the temperature of fluid increases with increasing of unsteady parameter $|A|$ for first and second solutions and consequently, the thickness of thermal boundary layer decreases.

The velocity and temperature profiles for different values of porosity parameter Λ are depicted in Figs. 12 and 13. From these figures, it is observed that the velocity and temperature profiles decrease with increasing Λ for both first and second solutions and consequently, the boundary layer thicknesses become thicker and thicker. It is also clear from these figures that the first solution displays a thinner boundary layer thickness compared to the second solution. Fig. 14 shows the temperature profiles for different values of radiation parameter N . It is seen from this figure that the temperature of fluid increases with N for first and second solutions and thus the thermal boundary layer thickness decreases. Actually, the radiative heat flux increases due to increasing values of N , because of that the thermal boundary layer thickness becomes thinner.

5 Conclusions

This paper examined the problem of an unsteady two-dimensional stagnation-point flow with melting heat transfer towards a flat plate immersed in a Darcy–Brinkman porous medium in the presence of thermal radiation. The existence of multiple solutions were clearly presented in the $(A, f''(0))$ and $(A, -\theta'(0))$ parameter spaces for various values of the melting parameter M and porosity parameter K . For the accelerating flow, the solution exists for all positive values of A , whereas for the decelerating flow, the solution exists up to a critical value $A_{\min} (< 0)$, which depends on M and K . The value $|A_{\min}|$ increases when the permeability parameter K increases, and this suggests that permeability increases the range of existence of the solutions. Meanwhile, the value $|A_{\min}|$ decreases with increasing values of M .

References

- [1] Bhattacharyya K, Mukhopadhyay S, Layek GC. Steady boundary layer slip flow and heat transfer over a flat porous plate embedded in a porous media. *J Petrol Sci Eng* 2011, 78, 304–309.
- [2] Pop I, Ingham DB. *Convective heat transfer: Mathematical and computational modelling of viscous fluids and porous media*. Pergamon, Oxford, 2001.

- [3] Ingham DB, Bejan A, Mamut E, Pop I. *Emerging Technologies and Techniques in Porous Media*. Kluwer, Dordrecht, 2004.
- [4] Bejan A, Dincer I, Lorente S, Miguel AF, Reis AH. *Porous and complex flow structures in modern technologies*. Springer, New York, 2004.
- [5] Vafai K. *Handbook of Porous Media*. 2nd ed., Taylor & Francis, New York, 2005.
- [6] Ingham DB, Pop I. *Transport Phenomena in Porous Media*. Elsevier, Oxford, 2005.
- [7] Nield DA, Bejan A. *Convection in porous media*, 3rd ed., Springer, New York, 2006.
- [8] P. Vadasz, "Emerging Topics in Heat and Mass Transfer in Porous Media. Springer, New York, 2008.
- [9] Ishak A, Nazar R, Pop I. Steady and unsteady boundary layer due to a stretching sheet in a porous medium using Darcy-Brinkman model. *Int J Appl Mech Eng* 2006, 11, 623–637.
- [10] Harris SD, Ingham DB, Pop I. Mixed convection boundary-layer flow near the stagnation point on a vertical surface in a porous medium: Brinkman model with slip. *Transport Porous Media* 2009, 77, 267–285.
- [11] Hamad MAA, Pop I. Scaling transformations for boundary layer flow near the stagnation-point on a heated permeable stretching surface in a porous medium saturated with a nanofluid and heat generation/absorption effects. *Transport Porous Media* 2010, DOI 10.1007/s11242-010-9683-8.
- [12] Rosali H, Ishak A, Pop I. Mixed convection stagnation-point flow over a vertical plate with prescribed heat flux embedded in a porous medium: Brinkman-extended Darcy formulation. *Transport Porous Media* 2011, DOI 10.1007/s11242-011-9809-7.
- [13] Pantokratoras A. Mixed convection in a Darcy–Brinkman porous medium with a constant convective thermal boundary condition. *Transport Porous Media* 2014, 104, 273–288.
- [14] Pantokratoras A. Forced convection in a Darcy–Brinkman porous medium with a convective thermal boundary condition. *J Porous Media* 2015, 18, 1–6.
- [15] Yacob NA, Ishak A, Pop I. Melting heat transfer in boundary layer stagnation-point flow towards a stretching/shrinking sheet in a micropolar fluid. *Computers Fluids*, 2011, 47, 16–21.
- [16] Epstein M, Cho DH. Melting heat transfer in steady laminar flow over a flat plate. *ASME J Heat Transfer* 1976, 98, 531–533.
- [17] Kazmierczak M, Poulikakos D, Pop I. Melting from a flat plate embedded in a porous medium in the presence of steady convection. *Numerical Heat Transfer* 1986, 10, 571–581.
- [18] Ishak A, Nazar R, Bachok N, Pop I. Melting heat transfer in steady laminar flow over a moving surface. *Heat Mass Transfer* 2010, 46, 463–468.
- [19] Hayat T, Mustafa M, Iqbal Z, Alsaedi A. Stagnation-point flow of couple stress fluid with melting heat transfer. *Appl Math Mech* 2013, 34, 167–176.
- [20] Ahmad S, Pop I. Melting effect on mixed convection boundary layer flow about a vertical surface embedded in a porous medium: Opposing flows case. *Transport Porous Media* 2014, 102, 317–323.
- [21] Mabood F, Mastroberardino A. Melting heat transfer on MHD convective flow of a nanofluid over a stretching sheet with viscous dissipation and second order slip. *J Taiwan Inst Chem Eng* 2015, 1–7.
- [22] Yang KT. Unsteady laminar boundary layers in an incompressible stagnation flow. *J Appl Mech* 1958, 25, 421–427.
- [23] Birkhoff G. *Hydrodynamics, a Study in Fact and Similitude*. Revised edn. Princeton University Press, Princeton, 1960.
- [24] Wang CY. Liquid film on an unsteady stretching surface. *Quart Appl Math* 1990, 48, 601–610.
- [25] Andersson HI, Aarseth JB, Dandapat BS. Heat transfer in a liquid film on an unsteady stretching surface. *Int J Heat Mass Transfer* 2000, 43, 69–74.
- [26] Ali ME, Magyari E. Unsteady fluid and heat flow induced by a submerged stretching surface while its steady motion is slowed down gradually. *Int J Heat Mass Transfer* 2007, 50, 1–2, 188–195.
- [27] Tie-Gang F, Ji Z, Shan-Shan Y. Viscous flow over an unsteady shrinking sheet with mass transfer. *Chin Phys Lett* 2009, 26, 014703-1–4.
- [28] Rohni AM, Ahmad S, Pop I, Merkin JH. Unsteady mixed convection boundary-layer flow with suction and temperature slip effects near the stagnation point on a vertical permeable surface embedded in a porous medium. *Transport Porous Media* 2012, 92, 1–14.
- [29] Sheremet MA, Trifonova TA. Unsteady conjugate natural convection in a vertical cylinder containing a horizontal porous layer: Darcy model and Brinkman-extended Darcy model. *Transport Porous Media* 2014, 101, 437–463.
- [30] Brewster MQ. *Thermal Radiative Transfer Properties*. John Wiley and Sons, 1972.
- [31] Weidman PD, Kubitschek DG, Davis AMJ. The effect of transpiration on self-similar boundary layer flow over moving surfaces. *Int J Eng Sci* 2006, 44, 730–737.
- [32] Roşca AV, Pop I. Flow and heat transfer over a vertical permeable stretching/shrinking sheet with a second order slip. *Int J Heat Mass Transfer* 2013, 60, 355–364.
- [33] Mahapatra TR, Nandy SK. Stability analysis of dual solutions in stagnation-point flow and heat transfer over a Power-law shrinking surface. *Int J Nonlinear Sci* 2011, 12, 86–94.
- [34] Nazar R, Noor A, Jafar K, Pop I. Stability analysis of three-dimensional flow and heat transfer over a permeable shrinking surface in a Cu-water nanofluid. *Int J Math Comput Physical Quantum Eng* 2014, 8, 776–782.
- [35] Hafidzuddin EH, Nazar R, Arifin NM, Pop I. Stability analysis of unsteady three-dimensional viscous flow over a permeable stretching/shrinking surface. *JQMA* 2015, 11, 19–31.
- [36] Harris SD, Ingham DB, Pop I. Mixed convection boundary-layer flow near the stagnation point on a vertical surface in a porous medium: Brinkman model with slip. *Transport Porous Media* 2009, 77, 267–285.
- [37] Yih KA. Uniform suction/blowing effect on forced convection about a wedge: uniform heat flux. *Acta Mech* 1998, 128, 173–181.
- [38] Ishak A, Nazar R, Pop I. Falkner-Skan equation for flow past a moving wedge with suction or injection. *J Appl Math Comp* 2007, 25, 67–83.